



# Estimation of Average Absorption Cross Section of a Skin Phantom in a mm-Wave Reverberation Chamber

Reza Aminzadeh, Jérôme Sol, Philippe Besnier, Maxim Zhadobov, Luc Martens, Wout Joseph

## ► To cite this version:

Reza Aminzadeh, Jérôme Sol, Philippe Besnier, Maxim Zhadobov, Luc Martens, et al.. Estimation of Average Absorption Cross Section of a Skin Phantom in a mm-Wave Reverberation Chamber. EUCAP 2019, Apr 2019, Krakow, Poland. hal-02133575

**HAL Id: hal-02133575**

**<https://hal.science/hal-02133575>**

Submitted on 18 May 2019

**HAL** is a multi-disciplinary open access archive for the deposit and dissemination of scientific research documents, whether they are published or not. The documents may come from teaching and research institutions in France or abroad, or from public or private research centers.

L'archive ouverte pluridisciplinaire **HAL**, est destinée au dépôt et à la diffusion de documents scientifiques de niveau recherche, publiés ou non, émanant des établissements d'enseignement et de recherche français ou étrangers, des laboratoires publics ou privés.

# Estimation of Average Absorption Cross Section of a Skin Phantom in a mm-Wave Reverberation Chamber

Reza Aminzadeh<sup>1\*</sup>, Jérôme Sol<sup>2</sup>, Philippe Besnier<sup>2</sup>, Maxim Zhadobov<sup>2</sup>, Luc Martens<sup>1</sup>, and Wout Joseph<sup>1</sup>

<sup>1</sup> Department of Information Technology, Ghent University/imec, B-9052 Ghent, Belgium

<sup>2</sup> University of Rennes, INSA Rennes, CNRS, IETR-UMR 6164, F-35000 Rennes 35708, France

\*email: reza.aminzadeh@ugent.be

**Abstract**—The average absorption cross section (AACS) of a human skin-equivalent phantom is calculated under diffuse exposure in a reverberation chamber (RC) in the mm-wave band. Two methods are proposed, in the first method the quality factor of the RC is evaluated in the spectral domain. The second method is based on the theory of room electromagnetics and fitting power delay profile to obtain reverberation time. Similar results were obtained for both methods. AACS values of  $225 \pm 0.048 \text{ cm}^2$  and  $225 \pm 0.017 \text{ cm}^2$  were derived for the first and second method, respectively. These results are in good agreement.

**Index Terms**—average absorption cross section, propagation, mm-wave, reverberation chamber, Q-factor, room electromagnetics.

## I. INTRODUCTION

The development of mm-wave applications e.g. mm-wave scanners, short-range high data rate communication systems has triggered a growing concern about potential health effects of mm-waves on human health [1]. Therefore, it is necessary to assess the thresholds of potential effects of mm-waves on biological tissues including in vivo and in vitro for humans as well as for animals [2], [3]. To this aim a mm-wave reverberation chamber (RC) could be used. Such RC facilitates generating statistically isotropic and homogeneous fields with high exposure levels. Using a mm-wave RC, radio-frequency absorption characteristics of small objects (i.e. tissue-equivalent phantoms, animals) could be investigated.

In this paper two methods are compared for calculation of the average absorption cross section (AACS) of a skin-equivalent phantom in a mm-wave RC in the 59.5-60.5 GHz range. In the first method, the AACS is derived based on the quality-factor of the RC while the second method estimates the AACS from the measured power delay profile and fitted reverberation time.

## II. METHODOLOGY

The AACS of the phantom is measured in the 59.5-60.5 GHz range. Two methods are presented to determine the AACS in the RC: (1) based on the measured Q-factor of the RC; and (2) using the room electromagnetics theory and reverberation time ( $\tau$ ) through fitting of the average power delay profile (APDP).

### A. Measurement Setup

The goal is to measure the AACS of a skin-equivalent phantom. The phantom ( $15 \times 15 \times 1 \text{ cm}^3$ ) has a complex permittivity of  $7.4 - j11.4$  (at 60 GHz) [4]. Fig. 1 depicts the proposed measurement setup in the mm-wave RC. The measurements are performed in a mm-wave RC. The RC is made of aluminum walls and has inner dimensions of  $0.58 \times 0.592 \times 0.595 \text{ m}^3$  [5]. The random fields inside the RC are generated using a metallic mode-stirrer through 100 positions of the stirrer during a full rotation. A WR-15 open-ended waveguide is used as transmitter (Tx) to generate the fields inside the RC. A four-patch single-layer antenna array [6] is used as the receiver (Rx). The Tx and Rx are connected to a ZVA 67 (Rohde&Schwarz, Munich, Germany) vector network analyzer (VNA). The VNA delivers a power of 1 mW to the Tx and measures the S-parameters of both antennas during the measurements.



Fig. 1. The proposed measurement setup in the mm-wave RC showing the Rx antenna (top) and the open-ended waveguide (bottom).

### B. Method 1: RC Q-factor

The Q-factor of the chamber is calculated from the S-parameters [7]:

$$Q(f) = \frac{16\pi^2 V}{\lambda^3} G(f) \quad (1)$$

where  $V$  is the volume of the chamber,  $\lambda$  is the wavelength,  $f$  is the frequency and  $G$  is the normalized transmission factor and is obtained from the S-parameters [8], [9]:

$$G(f) = \frac{\langle |S_{21}|^2 - |\langle S_{21} \rangle|^2 \rangle}{(1 - |\langle S_{11} \rangle|^2)(1 - |\langle S_{22} \rangle|^2) \eta_e \eta_r} \quad (2)$$

where  $|S_{21}|$  is the magnitude of forward transmission coefficient.  $S_{11}$ ,  $S_{22}$ ,  $\eta_e$  and  $\eta_r$  are the reflection coefficients of the transmitting and receiving antennas and the radiation efficiencies of the Tx and the Rx, respectively. The average over the stirrer's positions is indicated by  $\langle \cdot \rangle$ . The term  $|\langle S_{21} \rangle|^2$  is used to take any direct or unstirred path during the measurements [9].

The AACS of the phantom is determined from the Q-factors of the loaded RC and the empty (unloaded) RC [8]:

$$AACS(f) = \frac{2\pi V}{\lambda} \left( \frac{1}{Q_{loaded}(f)} - \frac{1}{Q_{empty}(f)} \right) \quad (3)$$

where  $Q_{loaded}$  and  $Q_{empty}$  are the Q factors for the loaded RC (the phantom is at least  $50\lambda$  far from both antennas) and empty (unloaded) RC, respectively.

### C. Method 2: Fitting power delay profile to obtain $\tau$

The reverberation time  $\tau$  in the RC is calculated from the slope of the linear tail of the time domain impulse response expressed in relative power (dB) [10], [11]:

$$\tau = -\frac{10 \log(e)}{\text{slope}} \quad (4)$$

where  $e = 2.718$  is the Euler's number and  $\text{slope}$  is the linear tail of the APDP. In order to determine the APDP in the RC, the squared modulus of the inverse Fourier transformation of the averaged  $S_{21}^{avg}(f)$  is calculated:

$$\begin{cases} S_{21}^{avg}(f) \xrightarrow{\mathcal{F}^{-1}} S_{21}^{avg}(t), \\ APDP(t) = 10 \log_{10}(|S_{21}^{avg}(t)|^2) \end{cases} \quad (5)$$

Next, a slope is fitted to the linear tail of APDP to determine  $\tau$  from eq (4). In practice, the APDP does not have a linear curve due to the noise level of the VNA, the applied inverse Fourier transform and measurement uncertainties. Therefore,  $\tau$  is derived over a certain delay or power range. Thus, the tail of APDP could be approximated by a straight line. Once the delay range is determined, a linear regression fit is applied to calculate the slope of the linear tail. An arbitrary noise floor is defined as 3 dB above the minimum APDP value.

Finally, the AACS is calculated as:

$$ACS = \frac{4V}{c} \left( \frac{1}{\tau_{loaded}} - \frac{1}{\tau_{empty}} \right) \quad (6)$$

where  $V$  is the volume of the chamber,  $c$  is the speed of light and  $\tau_{loaded}$  and  $\tau_{empty}$  are the reverberation times for the loaded RC and empty (unloaded) RC, respectively. Similar to

method 1 (Section II-B) the phantom is at least  $50\lambda$  far from both antennas.

## III. RESULTS AND DISCUSSION

Fig. 2 shows the measured Q-factor of the RC. For the empty RC a Q-factor in the range of 19000 to 30000 is measured. When the RC is loaded with the phantom the Q-factor decreases to the range of 6166 to 9962. At 60 GHz, the Q-factors of RC are 8237 and 24020 for the empty and loaded RC, respectively. Although the Q-factor of RC decreased due to the presence of the load in the RC, these values are still high enough to ensure the functionality of the RC.

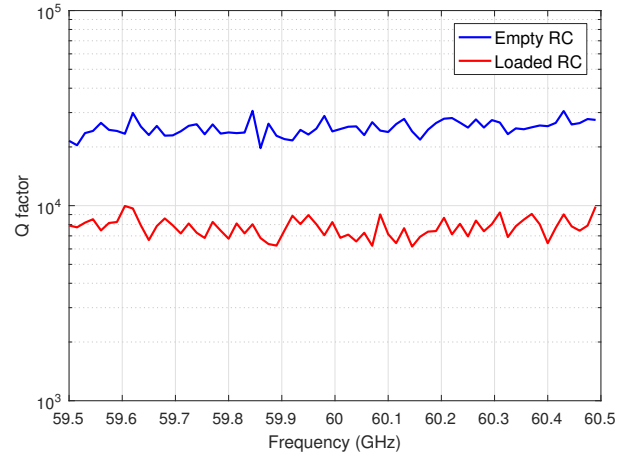


Fig. 2. The measured Q-factor of empty and loaded RC averaged over 100 positions of the stirrer.

Fig. 3 demonstrates the measured APDPs for the empty and loaded RC as well as the fitted slopes. For the loaded RC the slope of the APDP is steeper due to the faster decay of the diffuse field's energy. Correlation coefficients of 0.987 and 0.983 are obtained for the fitted slope to the linear tail of APDP for the empty RC and loaded RC, respectively, which shows an excellent fit of the slopes to the linear tail of the APDP. For the empty RC, a slope of -0.025 dB/ns is calculated while a slope of -0.061 dB/ns is obtained for the loaded RC. These values correspond to  $\tau$  values of 173.7 ns and 71.18 ns for the empty RC and loaded RC, respectively.

Fig. 4 illustrates the calculated AACS from Q-factor versus the calculated AACS from reverberation time for the skin phantom. The results of both methods are in very good agreement. In addition, a line is fitted to each of the AACS estimates as a function of frequency. At 60 GHz considering the Q-factor an AACS of  $225 \pm 0.048 \text{ cm}^2$  is obtained while the calculated AACS from  $\tau$  is about  $225 \pm 0.017 \text{ cm}^2$ . This is an excellent agreement compared to the dimensions of the phantom ( $15 \times 15 \text{ cm}^2$ ). The results show that both methods are in good agreement and could be used interchangeably to determine the AACS of the skin phantom in the RC at 60 GHz.

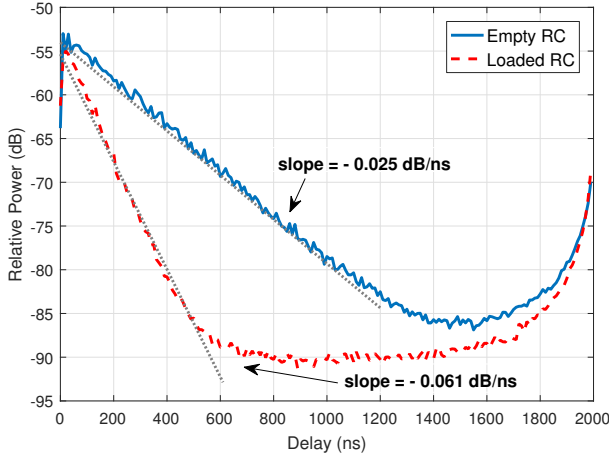


Fig. 3. Measured APDP of loaded and empty RC.

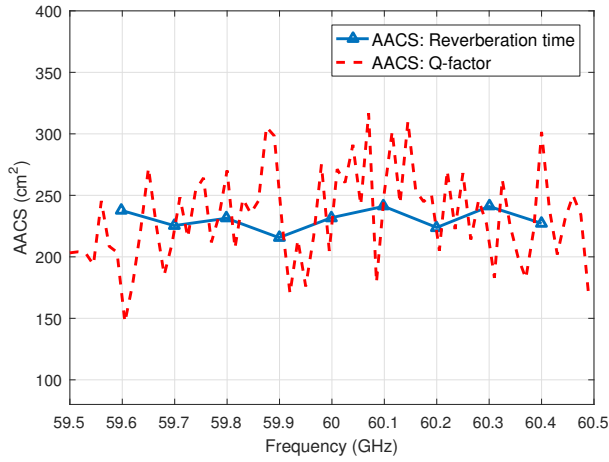


Fig. 4. Comparison of phantom's AACS: determined from Q-factor vs. reverberation time.

#### IV. CONCLUSION

This paper compares two methods for calculation of the average absorption cross section (AACS) of a skin-equivalent phantom in a mm-wave reverberation chamber (RC) in the 59.5-60.5 GHz range. The first method considers the quality factor of the RC while the second method considers fitting the average power delay profile to obtain the reverberation time and is based on the theory of room electromagnetics. The results of both methods are in good agreement, suggesting that they could be used to determine the AACS of the skin phantom in the RC in the mm-wave band. AACS values of  $225 \pm 0.048 \text{ cm}^2$  and  $225 \pm 0.017 \text{ cm}^2$  were derived either from the RC Q-factor estimation in the frequency domain or from the reverberation time (decay time constant) estimated through inverse Fourier transformation. Both methods use the same set of data and the results are in excellent agreement compared to the physical geometry of the phantom.

#### ACKNOWLEDGMENT

This research was funded by the Research Foundation Flanders (FWO) under grant agreement No G003415N.

#### REFERENCES

- [1] T. Wu, T. S. Rappaport, and C. M. Collins, "Safe for generations to come: Considerations of safety for millimeter waves in wireless communications," *IEEE Microwave Magazine*, vol. 16, no. 2, pp. 65–84, March 2015.
- [2] S. Koyama, E. Narita, Y. Shimizu, Y. Suzuki, T. Shiina, M. Taki, N. Shinohara, and J. Miyakoshi, "Effects of long-term exposure to 60 ghz millimeter-wavelength radiation on the genotoxicity and heat shock protein (Hsp) expression of cells derived from human eye," *International Journal of Environmental Research and Public Health*, vol. 13, no. 8, 2016.
- [3] A. J. Haas, Y. Le Page, M. Zhadobov, R. Sauleau, Y. L. Dréan, and C. Saligaut, "Effect of acute millimeter wave exposure on dopamine metabolism of NGF-treated PC12 cells," *Journal of Radiation Research*, vol. 58, no. 4, pp. 439–445, 2017.
- [4] R. Aminzadeh, A. K. Fall, J. Sol, A. Thielens, P. Besnier, M. Zhadobov, N. De Geeter, P. P. Vasudevan, L. Dupré, R. Van Holen, L. Martens, and W. Joseph, "Design and calibration of a mm-wave personal exposure meter for 5G exposure assessment in indoor diffuse environments," *Journal of Infrared, Millimeter, and Terahertz Waves*, Aug 2018.
- [5] A. K. Fall, P. Besnier, C. Lemoine, M. Zhadobov, and R. Sauleau, "Design and experimental validation of a mode-stirred reverberation chamber at millimeter waves," *IEEE Transactions on Electromagnetic Compatibility*, vol. 57, no. 1, pp. 12–21, Feb 2015.
- [6] N. Chahat, M. Zhadobov, L. L. Coq, S. I. Alekseev, and R. Sauleau, "Characterization of the interactions between a 60-GHz antenna and the human body in an off-body scenario," *IEEE Transactions on Antennas and Propagation*, vol. 60, no. 12, pp. 5958–5965, Dec 2012.
- [7] D. A. Hill, M. T. Ma, A. R. Ondrejka, B. F. Riddle, M. L. Crawford, and R. T. Johnk, "Aperture excitation of electrically large, lossy cavities," *IEEE Transactions on Electromagnetic Compatibility*, vol. 36, no. 3, pp. 169–178, Aug 1994.
- [8] D. Senić, C. Holloway, J. Ladbury, G. Koepke, and A. Šarolić, "Absorption characteristics and SAR of a lossy sphere inside a reverberation chamber," in *2014 International Symposium on Electromagnetic Compatibility*, Sept 2014, pp. 962–967.
- [9] P. Besnier, C. Lemoine, and J. Sol, "Various estimations of composite Q-factor with antennas in a reverberation chamber," in *2015 IEEE International Symposium on Electromagnetic Compatibility (EMC)*, Aug 2015, pp. 1223–1227.
- [10] J. B. Andersen, J. Ø. Nielsen, G. F. Pedersen, G. Bauch, and J. M. Herdin, "Room electromagnetics," *IEEE Antennas and Propagation Magazine*, vol. 49, no. 2, pp. 27–33, April 2007.
- [11] A. Bamba, W. Joseph, J. B. Andersen, E. Tanghe, G. Vermeeren, D. Plets, J. Ø. Nielsen, and L. Martens, "Experimental assessment of specific absorption rate using room electromagnetics," *IEEE Transactions on Electromagnetic Compatibility*, vol. 54, no. 4, pp. 747–757, Aug 2012.